INTERNATIONAL JOURNAL FOR NUMERICAL METHODS IN ENGINEERING
Int. J. Numer. Meth. Engng 2008; **73**:1251–1273
Published online 23 July 2007 in Wiley InterScience (www.interscience.wiley.com). DOI: 10.1002/nme.2118

Regularized meshless method for antiplane shear problems with multiple inclusions

K. H. Chen[1,*,†], J. T. Chen[2] and J. H. Kao[2]

[1]*Department of Civil Engineering, National Ilan University, Ilan 260, Taiwan*
[2]*Department of Harbor and River Engineering, National Taiwan Ocean University, Keelung 20224, Taiwan*

SUMMARY

In this paper, we employ the regularized meshless method to solve antiplane shear problems with multiple inclusions. The solution is represented by a distribution of double-layer potentials. The singularities of kernels are regularized by using a subtracting and adding-back technique. Therefore, the troublesome singularity in the method of fundamental solutions (MFS) is avoided and the diagonal terms of influence matrices are determined. An inclusion problem is decomposed into two parts: one is the exterior problem for a matrix with holes subjected to remote shear, the other is the interior problem for each inclusion. The two boundary densities, essential and natural data, along the interface between the inclusion and matrix satisfy the continuity and equilibrium conditions. A linear algebraic system is obtained by matching boundary conditions and interface conditions. Finally, numerical results demonstrate the accuracy of the present solution. Good agreements are obtained and compare well with analytical solutions and Gong's results. Copyright © 2007 John Wiley & Sons, Ltd.

Received 25 July 2006; Revised 13 March 2007; Accepted 8 May 2007

KEY WORDS: antiplane shear; elastic; inclusion; MFS; regularized meshless method; hypersingularity; displacement field

1. INTRODUCTION

Engineering materials always contain some defects in the form of inclusions or second-phase particles. The distribution of stress in an infinite medium containing inclusions under antiplane shear has been studied by many investigators [1–10]. In 1967, Goree and Wilson [6] presented numerical results for an infinite medium containing two inclusions under remote shear. Besides, Sendeckyj [8] proposed an iterative scheme for solving problems with multiple inclusions in 1971.

*Correspondence to: K. H. Chen, Department of Civil Engineering, National Ilan University, Ilan 260, Taiwan.
†E-mail: khc6177@yahoo.com.tw

Contract/grant sponsor: National Science Council; contract/grant number: NSC-95-2221-E-464-003-MY3

In addition, analytical solutions for two identical holes and inclusions were obtained by Stief [9] and by Budiansky and Carrier [2], respectively. Zimmerman [10] employed the Schwartz alternative method [8] for plane problems with two holes or inclusions to obtain a closed-form solution. In 1992, Honein *et al.* [7] derived the analytical solution for two unequal inclusions perfectly bonded to an infinite elastic matrix under antiplane shear. The solution was obtained *via* iterations of Möbius transformations involving the complex potential [7]. On the other hand, Bird and Steele [1] used a Fourier series procedure to revisit the antiplane elasticity problems of Honein *et al.* [7]. For a triangle pattern of three inclusions under antiplane shear, Gong [5] derived the general solution by employing complex potentials and the Laurent series expansion method in 1995. Based on the technique of analytical continuity and the method of successive approximation, Chao and Young [3] studied the stress concentration on a hole surrounded by two inclusions. Recently, Chen and Wu [4] have successfully solved the antiplane problem with circular holes and/or inclusions by using the boundary integral equation in conjunction with degenerate kernel and Fourier series. In this study, we will bring a meshless method systematically for multiple inclusions under antiplane shear.

The meshless implementation of the local boundary integral equation [11, 12], boundary knot method [13–15], boundary collocation method [16–18], non-dimensional dynamic influence functions method [19, 20] and method of fundamental solutions (MFS) [21–27] are several important meshless methods belonging to a boundary method for solving boundary value problems, which can be viewed as a discrete type of the indirect boundary element method [16]. To our knowledge, one of the very important meshless methods is the boundary collocation method [16–18, 28, 29]. Instead of using the singular fundamental solutions, the non-singular kernels were employed to evaluate the homogeneous solution for solving partial differential equations. In the MFS, the solution is approximated by a set of fundamental solutions, which are expressed in terms of sources located outside the physical domain. The unknown coefficients in the linear combination of the fundamental solutions, are determined by matching the boundary condition. The method is relatively easy to implement. It is adaptive in the sense that it can take into account sharp changes in the solution and in the geometry of the domain and can easily handle complex boundary conditions. A survey of the MFS and related methods over the last 30 years has been found [25–27]. However, the MFS is still not a popular method because of the debatable artificial boundary distance of source location in numerical implementation, especially for complicated geometry. The diagonal coefficients of influence matrices are divergent in the conventional case when the fictitious boundary approaches the physical boundary. In spite of its gain of singularity free, the influence matrices become ill-posed when the fictitious boundary is far away from the physical boundary. It results in an ill-posed problem since the condition number for the influence matrix becomes very large.

Recently, we developed a modified MFS, namely the regularized meshless method (RMM), to overcome the drawback of MFS for solving the simply connected and multiply connected Laplace problem [30, 31]. The method eliminates the well-known drawback of equivocal artificial boundary. The subtracting and adding-back technique [30–32] is implemented to regularize the singularity and hypersingularity of the kernel functions. This method can simultaneously distribute the observation and source points on the physical boundary even when using the singular kernels instead of non-singular kernels. The diagonal terms of the influence matrices can be extracted by using the proposed technique. Following the successful experiences in References [30, 31] for potential problems, this paper extends the developed meshless method (RMM) to carry out numerical results systematically for an infinite medium containing multiple inclusions (multi-domain) under

DOI: 10.1002/nme

antiplane shear. References [30, 31] were limited to simply connected and multiply connected problems, the purpose of this paper is to solve the multi-domain problems with various material properties by employing the RMM in conjunction with the domain decomposition technique. We have proposed a general algorithm for the stress fields around circular holes or inclusions. The method shows great generality and versatility for the problem.

In this paper, the RMM is provided to solve the antiplane shear problem with multiple inclusions. A general-purpose program was developed to solve antiplane shear problems with arbitrary number of inclusions. The results are compared with analytical solutions [7] and those of the Laurent series expansion method [5]. Furthermore, the stress concentration for different shear modulus ratio will be studied through several examples to show the validity of our method.

2. FORMULATION

2.1. Governing equation and boundary conditions

Consider the inclusions embedded in an infinite matrix as shown in Figure 1. The inclusions and the matrix have different elastic material properties. The matrix is subject to a remote antiplane shear, $\sigma_{zy} = \tau$. The displacement field of the antiplane deformation is defined as follows:

$$u = v = 0, \quad w = w(x, y) \tag{1}$$

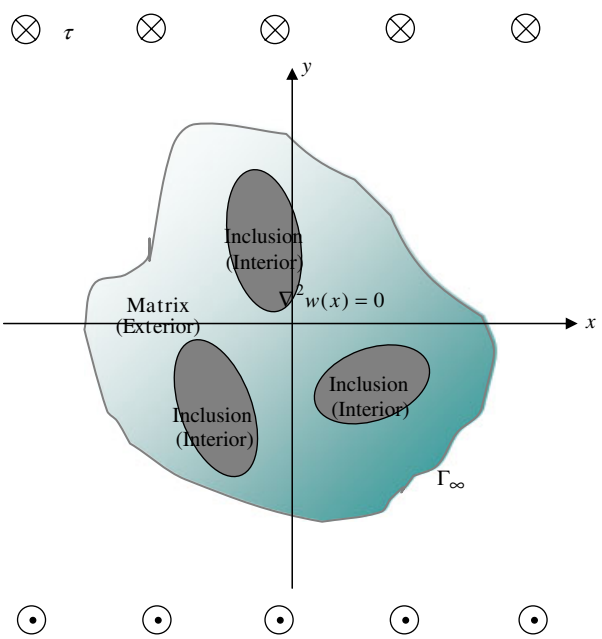

Figure 1. Problem sketch for a multiple inclusion problem under remote shear.

DOI: 10.1002/nme

where w is the function of x and y. For a linear elastic body, the stress components are

$$\sigma_{xz} = \sigma_{zx} = \mu \frac{\partial w}{\partial x} \tag{2}$$

$$\sigma_{yz} = \sigma_{zy} = \mu \frac{\partial w}{\partial y} \tag{3}$$

where μ is the shear modulus. The equilibrium equation can be simplified to

$$\frac{\partial \sigma_{zx}}{\partial x} + \frac{\partial \sigma_{zy}}{\partial y} = 0 \tag{4}$$

Substituting Equations (2) and (3) into (4), we have

$$\frac{\partial^2 w}{\partial x^2} + \frac{\partial^2 w}{\partial y^2} = \nabla^2 w = 0 \tag{5}$$

The continuity equilibrium conditions across the interface of the matrix–inclusion are described as

$$w^{\mathrm{m}} = w^{\mathrm{i}} \tag{6}$$

$$\mu^{\mathrm{m}} \frac{\partial w^{\mathrm{m}}}{\partial n} = -\mu^{\mathrm{i}} \frac{\partial w^{\mathrm{i}}}{\partial n} \tag{7}$$

where the superscripts i and m denote the inclusion and the matrix, respectively. The loading is remote shear.

2.2. Methodology

2.2.1. Review of conventional method of fundamental solutions. By employing the RBF technique [28, 29, 33–39], the representation of the solution in Equation (5) for the multiple-inclusion problem as shown in Figure 1, can be approximated in terms of the strengths α_j of the singularities as s_j as

$$\begin{aligned} w(x_i) &= \sum_{j=1}^{N} T(s_j, x_i)\alpha_j \\ &= \sum_{j=1}^{N_1} T(s_j, x_i)\alpha_j + \sum_{j=N_1+1}^{N_1+N_2} T(s_j, x_i)\alpha_j + \cdots + \sum_{j=N_1+N_2+\cdots+N_{m-1}+1}^{N} T(s_j, x_i)\alpha_j \end{aligned} \tag{8}$$

and

$$\begin{aligned} \frac{\partial w(x_i)}{\partial n_{x_i}} &= \sum_{j=1}^{N} M(s_j, x_i)\alpha_j \\ &= \sum_{j=1}^{N_1} M(s_j, x_i)\alpha_j + \sum_{j=N_1+1}^{N_1+N_2} M(s_j, x_i)\alpha_j + \cdots + \sum_{j=N_1+N_2+\cdots+N_{m-1}+1}^{N} M(s_j, x_i)\alpha_j \end{aligned} \tag{9}$$

DOI: 10.1002/nme

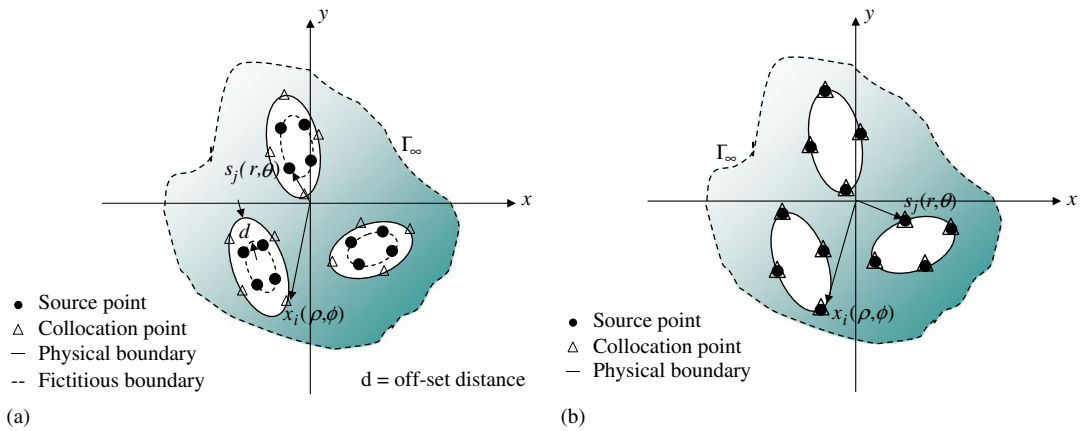

Figure 2. The distribution of the source points and observation points and definitions of r, θ, ρ, ϕ by using the conventional MFS and the RMM for the multi-domain problems: (a) conventional MFS and (b) RMM.

where $T(s_j, x_i)$ is a bivariate function of double-layer potential, x_i and s_j represent the ith observation point and the jth source point, respectively, α_j are the jth unknown coefficients (strength of the singularity), $N_1, N_2, \ldots, N_m$ are the numbers of source points on m number of boundaries of inclusions, respectively, while N is the total number of source points ($N = N_1 + N_2 + \cdots + N_m$) and $M(s_j, x_i) = \partial T(s_j, x_i)/\partial n_{x_i}$. After boundary conditions are satisfied at the boundary points, the coefficients $\{\alpha_j\}_{j=1}^{N}$ can be determined. The distributions of source points and observation points are shown in Figure 2(a) for the MFS. The chosen bases are the double-layer potentials [30, 31]:

$$T(s_j, x_i) = \frac{-\langle (x_i - s_j), n_j \rangle}{r_{ij}^2} \tag{10}$$

$$M(s_j, x_i) = \frac{2\langle (x_i - s_j), n_j \rangle \langle (x_i - s_j), \overline{n_i} \rangle}{r_{ij}^4} - \frac{\langle n_j, \overline{n_i} \rangle}{r_{ij}^2} \tag{11}$$

where $\langle\ ,\ \rangle$ is the inner product of two vectors, r_{ij} is $|s_j - x_i|$, n_j is the normal vector at s_j and $\overline{n_i}$ is the normal vector at x_i.

It is noted that the double-layer potentials have both singularity and hypersingularity when source and field points coincide, which leads to difficulty in the conventional MFS. The fictitious distance, d, between the fictitious (auxiliary) boundary (B') and the physical boundary (B) as shown in Figure 2(a) need to be chosen deliberately. To overcome the above-mentioned shortcoming, s_j is distributed on the physical boundary as shown in Figure 2(b), by using the proposed regularized technique as given in Section 2.2.2. The rationale for choosing double-layer potentials instead of single-layer potentials as the form of RBFs is to take advantage of the regularization of the subtracting and adding-back technique, so that no fictitious distance is needed when evaluating the diagonal coefficients of influence matrices that will be elaborated later in

DOI: 10.1002/nme

Section 2.2.3. If the single-layer potential is chosen as RBF, the regularization of the subtracting and adding-back technique fails because Equations (13), (16), (19) and (22) in Section 2.2.2 are not satisfied.

2.2.2. Regularized meshless method. The antiplane shear problem with multiple inclusions is decomposed into two problems as shown in Figure 3. One is the exterior problem for the matrix with holes subject to remote shear and the other is the interior problem for each inclusion. The two-boundary data between the matrix and the inclusion satisfy the continuity and equilibrium conditions in Equations (6) and (7). Furthermore, the exterior problem for the matrix can be superimposed by two systems as shown in Figure 4. One is the matrix with no hole subject to remote shear and the other is the matrix with holes. The representations of the two solutions for the interior problem ($w(x_i^{\mathrm{I}})$) and the exterior problem ($w(x_i^{\mathrm{O}})$) can be solved by using the RMM as follows:

(1) Interior problem: When the collocation point x_i approaches the source point s_j, the kernels in Equations (8) and (9) become singular. Equations (8) and (9) for the multiply connected problem as shown in Figure 2(b) need to be regularized by using the regularization of the subtracting and

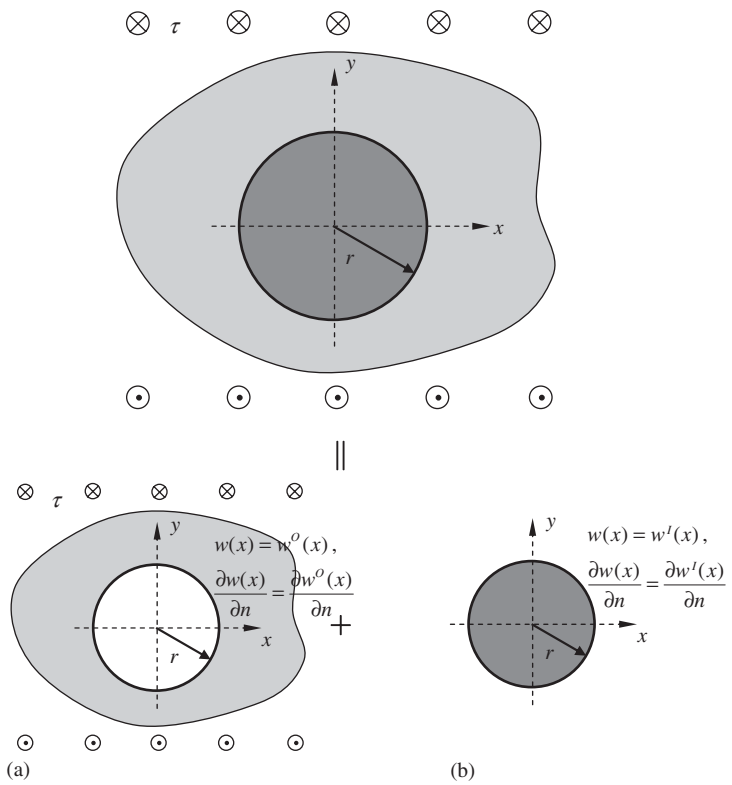

Figure 3. Decomposition of the problem.

DOI: 10.1002/nme

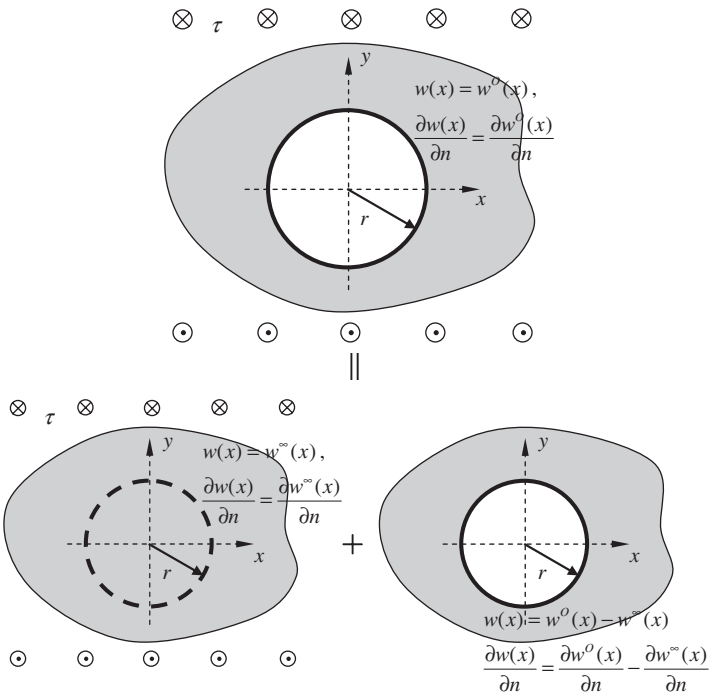

Figure 4. Decomposition of the problem of Figure 3(a).

adding-back technique [30–32] as follows:

$$w(x_i^{\mathrm{I}}) = \sum_{j=1}^{N_1} T(s_j^{\mathrm{I}}, x_i^{\mathrm{I}})\alpha_j + \cdots + \sum_{j=N_1+\cdots+N_{p-1}+1}^{N_1+\cdots+N_p} T(s_j^{\mathrm{I}}, x_i^{\mathrm{I}})\alpha_j$$

$$+ \cdots + \sum_{j=N_1+\cdots+N_{m-2}+1}^{N_1+\cdots+N_{m-1}} T(s_j^{\mathrm{I}}, x_i^{\mathrm{I}})\alpha_j + \sum_{j=N_1+\cdots+N_{m-1}+1}^{N} T(s_j^{\mathrm{I}}, x_i^{\mathrm{I}})\alpha_j$$

$$- \sum_{j=N_1+\cdots+N_{p-1}+1}^{N_1+\cdots+N_p} T(s_j^{\mathrm{I}}, x_i^{\mathrm{I}})\alpha_i, \quad x_i^{\mathrm{I}} \in B_p, \quad p = 1, 2, 3, \ldots, m \tag{12}$$

in which

$$\sum_{j=N_1+\cdots+N_{p-1}+1}^{N_1+\cdots+N_p} T(s_j^{\mathrm{I}}, x_i^{\mathrm{I}}) = 0, \quad x_i^{\mathrm{I}} \in B_p, \quad p = 1, 2, 3, \ldots, m \tag{13}$$

where m is the total number of boundaries. The superscript I and subscript p denote the interior problem and the pth boundary, respectively. The detailed derivation of Equation (13) is given in

DOI: 10.1002/nme

Reference [31]. Therefore, we can obtain

$$w(x_i^{\mathrm{I}}) = \sum_{j=1}^{N_1} T(s_j^{\mathrm{I}}, x_i^{\mathrm{I}})\alpha_j + \cdots + \sum_{j=N_1+\cdots+N_{p-1}+1}^{i-1} T(s_j^{\mathrm{I}}, x_i^{\mathrm{I}})\alpha_j$$

$$+ \sum_{j=i+1}^{N_1+\cdots+N_p} T(s_j^{\mathrm{I}}, x_i^{\mathrm{I}})\alpha_j + \cdots + \sum_{j=N_1+\cdots+N_{m-2}+1}^{N_1+\cdots+N_{m-1}} T(s_j^{\mathrm{I}}, x_i^{\mathrm{I}})\alpha_j$$

$$+ \sum_{j=N_1+\cdots+N_{m-1}+1}^{N} T(s_j^{\mathrm{I}}, x_i^{\mathrm{I}})\alpha_j - \left[\sum_{j=N_1+\cdots+N_{p-1}+1}^{N_1+\cdots+N_p} T(s_j^{\mathrm{I}}, x_i^{\mathrm{I}}) - T(s_i^{\mathrm{I}}, x_i^{\mathrm{I}}) \right] \alpha_i$$

$$x_i^{\mathrm{I}} \in B_p, \quad p = 1, 2, 3, \ldots, m \tag{14}$$

Similarly, the boundary flux is obtained as

$$\frac{\partial w(x_i^{\mathrm{I}})}{\partial n_{x_i^{\mathrm{I}}}} = \sum_{j=1}^{N_1} M(s_j^{\mathrm{I}}, x_i^{\mathrm{I}})\alpha_j + \cdots + \sum_{j=N_1+\cdots+N_{p-1}+1}^{N_1+\cdots+N_p} M(s_j^{\mathrm{I}}, x_i^{\mathrm{I}})\alpha_j$$

$$+ \cdots + \sum_{j=N_1+\cdots+N_{m-2}+1}^{N_1+\cdots+N_{m-1}} M(s_j^{\mathrm{I}}, x_i^{\mathrm{I}})\alpha_j + \sum_{j=N_1+\cdots+N_{m-1}+1}^{N} M(s_j^{\mathrm{I}}, x_i^{\mathrm{I}})\alpha_j$$

$$- \sum_{j=N_1+\cdots+N_{p-1}+1}^{N_1+\cdots+N_p} M(s_j^{\mathrm{I}}, x_i^{\mathrm{I}})\alpha_i, \quad x_i^{\mathrm{I}} \in B_p, \quad p = 1, 2, 3, \ldots, m \tag{15}$$

in which

$$\sum_{j=N_1+\cdots+N_{p-1}+1}^{N_1+\cdots+N_p} M(s_j^{\mathrm{I}}, x_i^{\mathrm{I}}) = 0, \quad x_i^{\mathrm{I}} \in B_p, \quad p = 1, 2, 3, \ldots, m \tag{16}$$

The detailed derivation of Equation (16) is also given in Reference [31]. Therefore, we obtain

$$\frac{\partial w(x_i^{\mathrm{I}})}{\partial n_{x_i^{\mathrm{I}}}} = \sum_{j=1}^{N_1} M(s_j^{\mathrm{I}}, x_i^{\mathrm{I}})\alpha_j + \cdots + \sum_{j=N_1+\cdots+N_{p-1}+1}^{i-1} M(s_j^{\mathrm{I}}, x_i^{\mathrm{I}})\alpha_j$$

$$+ \sum_{j=i+1}^{N_1+\cdots+N_p} M(s_j^{\mathrm{I}}, x_i^{\mathrm{I}})\alpha_j + \cdots + \sum_{j=N_1+\cdots+N_{m-2}+1}^{N_1+\cdots+N_{m-1}} M(s_j^{\mathrm{I}}, x_i^{\mathrm{I}})\alpha_j$$

$$+ \sum_{j=N_1+\cdots+N_{m-1}+1}^{N} M(s_j^{\mathrm{I}}, x_i^{\mathrm{I}})\alpha_j - \left[\sum_{j=N_1+\cdots+N_{p-1}+1}^{N_1+\cdots+N_p} M(s_j^{\mathrm{I}}, x_i^{\mathrm{I}}) - M(s_i^{\mathrm{I}}, x_i^{\mathrm{I}}) \right] \alpha_i$$

$$x_i^{\mathrm{I}} \in B_p, \quad p = 1, 2, 3, \ldots, m \tag{17}$$

DOI: 10.1002/nme

(2) Exterior problem: When the observation point x_i^{O} locates on the boundaries B_p, $p = 1, 2, 3, \ldots, m$, Equation (12) becomes

$$w(x_i^{\mathrm{O}}) = \sum_{j=1}^{N_1} T(s_j^{\mathrm{O}}, x_i^{\mathrm{O}})\alpha_j + \cdots + \sum_{j=N_1+\cdots+N_{P-1}+1}^{N_1+\cdots+N_p} T(s_j^{\mathrm{O}}, x_i^{\mathrm{O}})\alpha_j$$

$$+ \cdots + \sum_{j=N_1+\cdots+N_{m-2}+1}^{N_1+\cdots+N_{m-1}} T(s_j^{\mathrm{O}}, x_i^{\mathrm{O}})\alpha_j + \sum_{j=N_1+\cdots+N_{m-1}+1}^{N} T(s_j^{\mathrm{O}}, x_i^{\mathrm{O}})\alpha_j$$

$$- \sum_{j=N_1+\cdots+N_{p-1}+1}^{N_1+\cdots+N_p} T(s_j^{\mathrm{I}}, x_i^{\mathrm{I}})\alpha_i, \quad x_i^{\mathrm{O\ or\ I}} \in B_p, \quad p = 1, 2, 3, \ldots, m \tag{18}$$

where x_i^{O} is also located on the boundaries B_p and O denotes the exterior problem. Hence, we obtain

$$w(x_i^{\mathrm{O}}) = \sum_{j=1}^{N_1} T(s_j^{\mathrm{O}}, x_i^{\mathrm{O}})\alpha_j + \cdots + \sum_{j=N_1+\cdots+N_{p-1}+1}^{i-1} T(s_j^{\mathrm{O}}, x_i^{\mathrm{O}})\alpha_j$$

$$+ \sum_{j=i+1}^{N_1+\cdots+N_p} T(s_j^{\mathrm{O}}, x_i^{\mathrm{O}})\alpha_j + \cdots + \sum_{j=N_1+\cdots+N_{m-2}+1}^{N_1+\cdots+N_{m-1}} T(s_j^{\mathrm{O}}, x_i^{\mathrm{O}})\alpha_j$$

$$+ \sum_{j=N_1+\cdots+N_{m-1}+1}^{N} T(s_j^{\mathrm{O}}, x_i^{\mathrm{O}})\alpha_j - \left[\sum_{j=N_1+\cdots+N_{p-1}+1}^{N_1+\cdots+N_p} T(s_j^{\mathrm{I}}, x_i^{\mathrm{I}}) - T(s_i^{\mathrm{O}}, x_i^{\mathrm{O}}) \right] \alpha_i$$

$$x_i^{\mathrm{O\ or\ I}} \in B_p, \quad p = 1, 2, 3, \ldots, m \tag{19}$$

Similarly, the boundary flux is obtained as

$$\frac{\partial w(x_i^{\mathrm{O}})}{\partial n_{x_i^{\mathrm{O}}}} = \sum_{j=1}^{N_1} M(s_j^{\mathrm{O}}, x_i^{\mathrm{O}})\alpha_j + \cdots + \sum_{j=N_1+\cdots+N_{p-1}+1}^{N_1+\cdots+N_p} M(s_j^{\mathrm{O}}, x_i^{\mathrm{O}})\alpha_j$$

$$+ \cdots + \sum_{j=N_1+\cdots+N_{m-2}+1}^{N_1+\cdots+N_{m-1}} M(s_j^{\mathrm{O}}, x_i^{\mathrm{O}})\alpha_j + \sum_{j=N_1+\cdots+N_{m-1}+1}^{N} M(s_j^{\mathrm{O}}, x_i^{\mathrm{O}})\alpha_j$$

$$- \sum_{j=N_1+\cdots+N_{p-1}+1}^{N_1+\cdots+N_p} M(s_j^{\mathrm{I}}, x_i^{\mathrm{I}})\alpha_i, \quad x_i^{\mathrm{O\ or\ I}} \in B_p, \quad p = 1, 2, 3, \ldots, m \tag{20}$$

DOI: 10.1002/nme

Hence, we obtain

$$\frac{\partial w(x_i^{\mathrm{O}})}{\partial n_{x_i^{\mathrm{O}}}} = \sum_{j=1}^{N_1} M(s_j^{\mathrm{O}}, x_i^{\mathrm{O}})\alpha_j + \cdots + \sum_{j=N_1+\cdots+N_{p-1}+1}^{i-1} M(s_j^{\mathrm{O}}, x_i^{\mathrm{O}})\alpha_j$$
$$+ \sum_{j=i+1}^{N_1+\cdots+N_p} M(s_j^{\mathrm{O}}, x_i^{\mathrm{O}})\alpha_j + \cdots + \sum_{j=N_1+\cdots+N_{m-2}+1}^{N_1+\cdots+N_{m-1}} M(s_j^{\mathrm{O}}, x_i^{\mathrm{O}})\alpha_j$$
$$+ \sum_{j=N_1+\cdots+N_{m-1}+1}^{N} M(s_j^{\mathrm{O}}, x_i^{\mathrm{O}})\alpha_j - \left[\sum_{j=N_1+\cdots+N_{p-1}+1}^{N_1+\cdots+N_p} M(s_j^{\mathrm{I}}, x_i^{\mathrm{I}}) - M(s_i^{\mathrm{O}}, x_i^{\mathrm{O}}) \right] \alpha_i$$
$$x_i^{\mathrm{O\ or\ I}} \in B_p, \quad p = 1, 2, 3, \ldots, m \tag{21}$$

According to the dependence of the normal vectors for inner and outer boundaries [31], their relationships are

$$\begin{aligned} T(s_j^{\mathrm{I}}, x_i^{\mathrm{I}}) &= -T(s_j^{\mathrm{O}}, x_i^{\mathrm{O}}), \quad i \neq j \\ T(s_j^{\mathrm{I}}, x_i^{\mathrm{I}}) &= T(s_j^{\mathrm{O}}, x_i^{\mathrm{O}}), \quad i = j \end{aligned} \tag{22}$$

$$\begin{aligned} M(s_j^{\mathrm{I}}, x_i^{\mathrm{I}}) &= M(s_j^{\mathrm{O}}, x_i^{\mathrm{O}}), \quad i \neq j \\ M(s_j^{\mathrm{I}}, x_i^{\mathrm{I}}) &= M(s_j^{\mathrm{O}}, x_i^{\mathrm{O}}), \quad i = j \end{aligned} \tag{23}$$

where the left-hand side and the right-hand side of the equal sign in Equations (22) and (23) denote the kernels for observation and source points with the inward and outward normal vectors, respectively.

By using the proposed technique, the singular terms in Equations (8) and (9) have been transformed into regular terms

$$-\left[\sum_{j=N_1+N_2+\cdots+N_{p-1}+1}^{N_1+N_2+\cdots+N_p} T(s_j^{\mathrm{I}}, x_i^{\mathrm{I}}) - T(s_i^{\mathrm{I\ or\ O}}, x_i^{\mathrm{I\ or\ O}}) \right] \quad \text{and}$$
$$-\left[\sum_{j=N_1+\cdots+N_{p-1}+1}^{N_1+\cdots+N_p} M(s_j^{\mathrm{I}}, x_i^{\mathrm{I}}) - M(s_i^{\mathrm{I\ or\ O}} x_i^{\mathrm{I\ or\ O}}) \right]$$

in Equations (14), (17), (19) and (21), respectively, where $p = 1, 2, 3, \ldots, m$. The terms $\sum_{j=N_1+\cdots+N_{p-1}+1}^{N_1+\cdots+N_p} T(s_j^{\mathrm{I}}, x_i^{\mathrm{I}})$ and $\sum_{j=N_1+\cdots+N_{p-1}+1}^{N_1+\cdots+N_p} M(s_j^{\mathrm{I}}, x_i^{\mathrm{I}})$ are the adding-back terms and the terms $T(s_i^{\mathrm{I\ or\ O}}, x_i^{\mathrm{I\ or\ O}})$ and $M(s_i^{\mathrm{I\ or\ O}}, x_i^{\mathrm{I\ or\ O}})$ are the subtracting terms in the two brackets for regularization. After using the above-mentioned method of regularization of the subtracting and adding-back technique [30–32], we are able to remove the singularity and hypersingularity of the kernel functions.

DOI: 10.1002/nme

2.2.3. Construction of influence matrices for arbitrary domain problems. (1) Interior problem (inclusion): From Equations (14) and (17), the linear algebraic system can be yielded as

$$\begin{Bmatrix} w_1 \\ \vdots \\ w_N \end{Bmatrix} = [T^{\mathrm{I}}] \begin{Bmatrix} \alpha_1 \\ \vdots \\ \alpha_N \end{Bmatrix} = \begin{bmatrix} [T^{\mathrm{I}}_{11}] & \cdots & [T^{\mathrm{I}}_{1N}] \\ \vdots & \ddots & \vdots \\ [T^{\mathrm{I}}_{N1}] & \cdots & [T^{\mathrm{I}}_{NN}] \end{bmatrix} \begin{Bmatrix} \alpha_1 \\ \vdots \\ \alpha_N \end{Bmatrix} \tag{24}$$

$$\begin{Bmatrix} \dfrac{\partial w_1}{\partial n} \\ \vdots \\ \dfrac{\partial w_N}{\partial n} \end{Bmatrix} = [M^{\mathrm{I}}] \begin{Bmatrix} \alpha_1 \\ \vdots \\ \alpha_N \end{Bmatrix} = \begin{bmatrix} [M^{\mathrm{I}}_{11}] & \cdots & [M^{\mathrm{I}}_{1N}] \\ \vdots & \ddots & \vdots \\ [M^{\mathrm{I}}_{N1}] & \cdots & [M^{\mathrm{I}}_{NN}] \end{bmatrix} \begin{Bmatrix} \alpha_1 \\ \vdots \\ \alpha_N \end{Bmatrix} \tag{25}$$

where

$$[T^{\mathrm{I}}_{11}] = \begin{bmatrix} -\left[\sum_{j=1}^{N_1} T(s^{\mathrm{I}}_j, x^{\mathrm{I}}_1) - T(s^{\mathrm{I}}_1, x^{\mathrm{I}}_1)\right] & T(s^{\mathrm{I}}_2, x^{\mathrm{I}}_1) & \cdots & T(s^{\mathrm{I}}_{N_1}, x^{\mathrm{I}}_1) \\ T(s^{\mathrm{I}}_1, x^{\mathrm{I}}_2) & -\left[\sum_{j=1}^{N_1} T(s^{\mathrm{I}}_j, x^{\mathrm{I}}_2) - T(s^{\mathrm{I}}_2, x^{\mathrm{I}}_2)\right] & \cdots & T(s^{\mathrm{I}}_{N_1}, x^{\mathrm{I}}_2) \\ \vdots & \vdots & \ddots & \vdots \\ T(s^{\mathrm{I}}_1, x^{\mathrm{I}}_{N_1}) & T(s^{\mathrm{I}}_2, x^{\mathrm{I}}_{N_1}) & \cdots & -\left[\sum_{j=1}^{N_1} T(s^{\mathrm{I}}_j, x^{\mathrm{I}}_{N_1}) - T(s^{\mathrm{I}}_{N_1}, x^{\mathrm{I}}_{N_1})\right] \end{bmatrix}_{N_1 \times N_1} \tag{26}$$

$$[T^{\mathrm{I}}_{1N}] = \begin{bmatrix} T(s^{\mathrm{I}}_{N_1+\cdots+N_{m-1}+1}, x^{\mathrm{I}}_1) & T(s^{\mathrm{I}}_{N_1+\cdots+N_{m-1}+2}, x^{\mathrm{I}}_1) & \cdots & T(s^{\mathrm{I}}_N, x^{\mathrm{I}}_1) \\ T(s^{\mathrm{I}}_{N_1+\cdots+N_{m-1}+1}, x^{\mathrm{I}}_2) & T(s^{\mathrm{I}}_{N_1+\cdots+N_{m-1}+2}, x^{\mathrm{I}}_2) & \cdots & T(s^{\mathrm{I}}_N, x^{\mathrm{I}}_2) \\ \vdots & \vdots & \ddots & \vdots \\ T(s^{\mathrm{I}}_{N_1+\cdots+N_{m-1}+1}, x^{\mathrm{I}}_{N_1}) & T(s^{\mathrm{I}}_{N_1+\cdots+N_{m-1}+2}, x^{\mathrm{I}}_{N_1}) & \cdots & T(s^{\mathrm{I}}_N, x^{\mathrm{I}}_{N_1}) \end{bmatrix}_{N_1 \times N_m} \tag{27}$$

$$[T^{\mathrm{I}}_{N1}] = \begin{bmatrix} T(s^{\mathrm{I}}_1, x^{\mathrm{I}}_{N_1+\cdots+N_{m-1}+1}) & T(s^{\mathrm{I}}_2, x^{\mathrm{I}}_{N_1+\cdots+N_{m-1}+1}) & \cdots & T(s^{\mathrm{I}}_{N_1}, x^{\mathrm{I}}_{N_1+\cdots+N_{m-1}+1}) \\ T(s^{\mathrm{I}}_1, x^{\mathrm{I}}_{N_1+\cdots+N_{m-1}+2}) & T(s^{\mathrm{I}}_2, x^{\mathrm{I}}_{N_1+\cdots+N_{m-1}+2}) & \cdots & T(s^{\mathrm{I}}_{N_1}, x^{\mathrm{I}}_{N_1+\cdots+N_{m-1}+2}) \\ \vdots & \vdots & \ddots & \vdots \\ T(s^{\mathrm{I}}_1, x^{\mathrm{I}}_N) & T(s^{\mathrm{I}}_2, x^{\mathrm{I}}_N) & \cdots & T(s^{\mathrm{I}}_{N_1}, x^{\mathrm{I}}_N) \end{bmatrix}_{N_m \times N_1} \tag{28}$$

DOI: 10.1002/nme

$$[T^{\mathrm{I}}_{NN}]$$

$$= \begin{bmatrix} -\left[\sum_{j=N_1+\cdots+N_{m-1}+1}^{N} T(s^{\mathrm{I}}_j, x^{\mathrm{I}}_{N_1+\cdots+N_{m-1}+1}) - T(s^{\mathrm{I}}_{N_1+\cdots+N_{m-1}+1}, x^{\mathrm{I}}_{N_1+\cdots+N_{m-1}+1})\right] & \cdots & T(s^{\mathrm{I}}_{N_1+\cdots+N_{m-1}+1}, x^{\mathrm{I}}_N) \\ \vdots & \ddots & \vdots \\ T(s^{\mathrm{I}}_N, x^{\mathrm{I}}_{N_1+\cdots+N_{m-1}+1}) & \cdots & -\left[\sum_{j=N_1+\cdots+N_{m-1}+1}^{N} T(s^{\mathrm{I}}_j, x^{\mathrm{I}}_N) - T(s^{\mathrm{I}}_N, x^{\mathrm{I}}_N)\right] \end{bmatrix}_{N_m \times N_m} \tag{29}$$

$$[M^{\mathrm{I}}_{11}] = \begin{bmatrix} -\left[\sum_{j=1}^{N_1} M(s^{\mathrm{I}}_j, x^{\mathrm{I}}_1) - M(s^{\mathrm{I}}_1, x^{\mathrm{I}}_1)\right] & M(s^{\mathrm{I}}_2, x^{\mathrm{I}}_1) & \cdots & M(s^{\mathrm{I}}_{N_1}, x^{\mathrm{I}}_1) \\ M(s^{\mathrm{I}}_1, x^{\mathrm{I}}_2) & -\left[\sum_{j=1}^{N_1} M(s^{\mathrm{I}}_j, x^{\mathrm{I}}_2) - M(s^{\mathrm{I}}_2, x^{\mathrm{I}}_2)\right] & \cdots & M(s^{\mathrm{I}}_{N_1}, x^{\mathrm{I}}_2) \\ \vdots & \vdots & \ddots & \vdots \\ M(s^{\mathrm{I}}_1, x^{\mathrm{I}}_{N_1}) & M(s^{\mathrm{I}}_2, x^{\mathrm{I}}_{N_1}) & \cdots & -\left[\sum_{j=1}^{N_1} M(s^{\mathrm{I}}_j, x^{\mathrm{I}}_{N_1}) - M(s^{\mathrm{I}}_{N_1}, x^{\mathrm{I}}_{N_1})\right] \end{bmatrix}_{N_1 \times N_1} \tag{30}$$

$$[M^{\mathrm{I}}_{1N}] = \begin{bmatrix} M(s^{\mathrm{I}}_{N_1+\cdots+N_{m-1}+1}, x^{\mathrm{I}}_1) & M(s^{\mathrm{I}}_{N_1+\cdots+N_{m-1}+2}, x^{\mathrm{I}}_1) & \cdots & M(s^{\mathrm{I}}_N, x^{\mathrm{I}}_1) \\ M(s^{\mathrm{I}}_{N_1+\cdots+N_{m-1}+1}, x^{\mathrm{I}}_2) & M(s^{\mathrm{I}}_{N_1+\cdots+N_{m-1}+2}, x^{\mathrm{I}}_2) & \cdots & M(s^{\mathrm{I}}_N, x^{\mathrm{I}}_2) \\ \vdots & \vdots & \ddots & \vdots \\ M(s^{\mathrm{I}}_{N_1+\cdots+N_{m-1}+1}, x^{\mathrm{I}}_{N_1}) & M(s^{\mathrm{I}}_{N_1+\cdots+N_{m-1}+2}, x^{\mathrm{I}}_{N_1}) & \cdots & M(s^{\mathrm{I}}_N, x^{\mathrm{I}}_{N_1}) \end{bmatrix}_{N_1 \times N_m} \tag{31}$$

$$[M^{\mathrm{I}}_{N1}] = \begin{bmatrix} M(s^{\mathrm{I}}_1, x^{\mathrm{I}}_{N_1+\cdots+N_{m-1}+1}) & M(s^{\mathrm{I}}_2, x^{\mathrm{I}}_{N_1+\cdots+N_{m-1}+1}) & \cdots & M(s^{\mathrm{I}}_{N_1}, x^{\mathrm{I}}_{N_1+\cdots+N_{m-1}+1}) \\ M(s^{\mathrm{I}}_1, x^{\mathrm{I}}_{N_1+\cdots+N_{m-1}+2}) & M(s^{\mathrm{I}}_2, x^{\mathrm{I}}_{N_1+\cdots+N_{m-1}+2}) & \cdots & M(s^{\mathrm{I}}_{N_1}, x^{\mathrm{I}}_{N_1+\cdots+N_{m-1}+2}) \\ \vdots & \vdots & \ddots & \vdots \\ M(s^{\mathrm{I}}_1, x^{\mathrm{I}}_N) & M(s^{\mathrm{I}}_2, x^{\mathrm{I}}_N) & \cdots & M(s^{\mathrm{I}}_{N_1}, x^{\mathrm{I}}_N) \end{bmatrix}_{N_m \times N_1} \tag{32}$$

$$[M^{\mathrm{I}}_{NN}]$$

$$= \begin{bmatrix} -\left[\sum_{j=N_1+\cdots+N_{m-1}+1}^{N} M(s^{\mathrm{I}}_j, x^{\mathrm{I}}_{N_1+\cdots+N_{m-1}+1}) - M(s^{\mathrm{I}}_{N_1+\cdots+N_{m-1}+1}, x^{\mathrm{I}}_{N_1+\cdots+N_{m-1}+1})\right] & \cdots & M(s^{\mathrm{I}}_{N_1+\cdots+N_{m-1}+1}, x^{\mathrm{I}}_N) \\ \vdots & \ddots & \vdots \\ M(s^{\mathrm{I}}_N, x^{\mathrm{I}}_{N_1+\cdots+N_{m-1}+1}) & \cdots & -\left[\sum_{j=N_1+\cdots+N_{m-1}+1}^{N} M(s^{\mathrm{I}}_j, x^{\mathrm{I}}_N) - M(s^{\mathrm{I}}_N, x^{\mathrm{I}}_N)\right] \end{bmatrix}_{N_m \times N_m} \tag{33}$$

DOI: 10.1002/nme

(2) Exterior problem (matrix): Equations (19) and (21) yield

$$\begin{Bmatrix} w_1 \\ \vdots \\ w_N \end{Bmatrix} = [T^{\mathrm{O}}] \begin{Bmatrix} \alpha_1 \\ \vdots \\ \alpha_N \end{Bmatrix} = \begin{bmatrix} [T_{11}^{\mathrm{O}}] & \cdots & [T_{1N}^{\mathrm{O}}] \\ \vdots & \ddots & \vdots \\ [T_{N1}^{\mathrm{O}}] & \cdots & [T_{NN}^{\mathrm{O}}] \end{bmatrix} \begin{Bmatrix} \alpha_1 \\ \vdots \\ \alpha_N \end{Bmatrix} \tag{34}$$

$$\begin{Bmatrix} \dfrac{\partial w_1}{\partial n} \\ \vdots \\ \dfrac{\partial w_N}{\partial n} \end{Bmatrix} = [M^{\mathrm{O}}] \begin{Bmatrix} \alpha_1 \\ \vdots \\ \alpha_N \end{Bmatrix} = \begin{bmatrix} [M_{11}^{\mathrm{O}}] & \cdots & [M_{1N}^{\mathrm{O}}] \\ \vdots & \ddots & \vdots \\ [M_{N1}^{\mathrm{O}}] & \cdots & [M_{NN}^{\mathrm{O}}] \end{bmatrix} \begin{Bmatrix} \alpha_1 \\ \vdots \\ \alpha_N \end{Bmatrix} \tag{35}$$

in which

$$[T_{11}^{\mathrm{O}}] = \begin{bmatrix} -\left[\sum_{j=1}^{N_1} T(s_j^{\mathrm{I}}, x_1^{\mathrm{I}}) - T(s_1^{\mathrm{O}}, x_1^{\mathrm{O}})\right] & T(s_2^{\mathrm{O}}, x_1^{\mathrm{O}}) & \cdots & T(s_{N_1}^{\mathrm{O}}, x_1^{\mathrm{O}}) \\ T(s_1^{\mathrm{O}}, x_2^{\mathrm{O}}) & -\left[\sum_{j=1}^{N_1} T(s_j^{\mathrm{I}}, x_2^{\mathrm{I}}) - T(s_2^{\mathrm{O}}, x_2^{\mathrm{O}})\right] & \cdots & T(s_{N_1}^{\mathrm{O}}, x_2^{\mathrm{O}}) \\ \vdots & \vdots & \ddots & \vdots \\ T(s_1^{\mathrm{O}}, x_{N_1}^{\mathrm{O}}) & T(s_2^{\mathrm{O}}, x_{N_1}^{\mathrm{O}}) & \cdots & -\left[\sum_{j=1}^{N_1} T(s_j^{\mathrm{I}}, x_{N_1}^{\mathrm{I}}) - T(s_{N_1}^{\mathrm{O}}, x_{N_1}^{\mathrm{O}})\right] \end{bmatrix}_{N_1 \times N_1} \tag{36}$$

$$[T_{1N}^{\mathrm{O}}] = \begin{bmatrix} T(s_{N_1+\cdots+N_{m-1}+1}^{\mathrm{O}}, x_1^{\mathrm{O}}) & T(s_{N_1+\cdots+N_{m-1}+2}^{\mathrm{O}}, x_1^{\mathrm{O}}) & \cdots & T(s_N^{\mathrm{O}}, x_1^{\mathrm{O}}) \\ T(s_{N_1+\cdots+N_{m-1}+1}^{\mathrm{O}}, x_2^{\mathrm{O}}) & T(s_{N_1+\cdots+N_{m-1}+2}^{\mathrm{O}}, x_2^{\mathrm{O}}) & \cdots & T(s_N^{\mathrm{O}}, x_2^{\mathrm{O}}) \\ \vdots & \vdots & \ddots & \vdots \\ T(s_{N_1+\cdots+N_{m-1}+1}^{\mathrm{O}}, x_{N_1}^{\mathrm{O}}) & T(s_{N_1+\cdots+N_{m-1}+2}^{\mathrm{O}}, x_{N_1}^{\mathrm{O}}) & \cdots & T(s_N^{\mathrm{O}}, x_{N_1}^{\mathrm{O}}) \end{bmatrix}_{N_1 \times N_m} \tag{37}$$

$$[T_{N1}^{\mathrm{O}}] = \begin{bmatrix} T(s_1^{\mathrm{O}}, x_{N_1+\cdots+N_{m-1}+1}^{\mathrm{O}}) & T(s_2^{\mathrm{O}}, x_{N_1+\cdots+N_{m-1}+1}^{\mathrm{O}}) & \cdots & T(s_{N_1}^{\mathrm{O}}, x_{N_1+\cdots+N_{m-1}+1}^{\mathrm{O}}) \\ T(s_1^{\mathrm{O}}, x_{N_1+\cdots+N_{m-1}+2}^{\mathrm{O}}) & T(s_2^{\mathrm{O}}, x_{N_1+\cdots+N_{m-1}+2}^{\mathrm{O}}) & \cdots & T(s_{N_1}^{\mathrm{O}}, x_{N_1+\cdots+N_{m-1}+2}^{\mathrm{O}}) \\ \vdots & \vdots & \ddots & \vdots \\ T(s_1^{\mathrm{O}}, x_N^{\mathrm{O}}) & T(s_2^{\mathrm{O}}, x_N^{\mathrm{O}}) & \cdots & T(s_{N_1}^{\mathrm{O}}, x_N^{\mathrm{O}}) \end{bmatrix}_{N_m \times N_1} \tag{38}$$

DOI: 10.1002/nme

$$[T^{\mathrm{O}}_{NN}]$$

$$= \begin{bmatrix} -\left[\sum_{j=N_1+\cdots+N_{m-1}+1}^{N} T(s_j^{\mathrm{I}}, x^{\mathrm{I}}_{N_1+\cdots+N_{m-1}+1}) - T(s^{\mathrm{O}}_{N_1+\cdots+N_{m-1}+1}, x^{\mathrm{O}}_{N_1+\cdots+N_{m-1}+1})\right] & \cdots & T(s^{\mathrm{O}}_{N_1+\cdots+N_{m-1}+1}, x^{\mathrm{O}}_{N}) \\ \vdots & \ddots & \vdots \\ T(s^{\mathrm{O}}_{N}, x^{\mathrm{O}}_{N_1+\cdots+N_{m-1}+1}) & \cdots & -\left[\sum_{j=N_1+\cdots+N_{m-1}+1}^{N} T(s_j^{\mathrm{I}}, x^{\mathrm{I}}_{N}) - T(s^{\mathrm{O}}_{N}, x^{\mathrm{O}}_{N})\right] \end{bmatrix}_{N_m \times N_m} \tag{39}$$

$$[M^{\mathrm{O}}_{11}] = \begin{bmatrix} -\left[\sum_{j=1}^{N_1} M(s_j^{\mathrm{I}}, x_1^{\mathrm{I}}) - M(s_1^{\mathrm{O}}, x_1^{\mathrm{O}})\right] & M(s_2^{\mathrm{O}}, x_1^{\mathrm{O}}) & \cdots & M(s^{\mathrm{O}}_{N_1}, x_1^{\mathrm{O}}) \\ M(s_1^{\mathrm{O}}, x_2^{\mathrm{O}}) & -\left[\sum_{j=1}^{N_1} M(s_j^{\mathrm{I}}, x_2^{\mathrm{I}}) - M(s_2^{\mathrm{O}}, x_2^{\mathrm{O}})\right] & \cdots & M(s^{\mathrm{O}}_{N_1}, x_2^{\mathrm{O}}) \\ \vdots & \vdots & \ddots & \vdots \\ M(s_1^{\mathrm{O}}, x^{\mathrm{O}}_{N_1}) & M(s_2^{\mathrm{O}}, x^{\mathrm{O}}_{N_1}) & \cdots & -\left[\sum_{j=1}^{N_1} M(s_j^{\mathrm{I}}, x^{\mathrm{I}}_{N_1}) - M(s^{\mathrm{O}}_{N_1}, x^{\mathrm{O}}_{N_1})\right] \end{bmatrix}_{N_1 \times N_1} \tag{40}$$

$$[M^{\mathrm{O}}_{1N}] = \begin{bmatrix} M(s^{\mathrm{O}}_{N_1+\cdots+N_{m-1}+1}, x_1^{\mathrm{O}}) & M(s^{\mathrm{O}}_{N_1+\cdots+N_{m-1}+2}, x_1^{\mathrm{O}}) & \cdots & M(s^{\mathrm{O}}_{N}, x_1^{\mathrm{O}}) \\ M(s^{\mathrm{O}}_{N_1+\cdots+N_{m-1}+1}, x_2^{\mathrm{O}}) & M(s^{\mathrm{O}}_{N_1+\cdots+N_{m-1}+2}, x_2^{\mathrm{O}}) & \cdots & M(s^{\mathrm{O}}_{N}, x_2^{\mathrm{O}}) \\ \vdots & \vdots & \ddots & \vdots \\ M(s^{\mathrm{O}}_{N_1+\cdots+N_{m-1}+1}, x^{\mathrm{O}}_{N_1}) & M(s^{\mathrm{O}}_{N_1+\cdots+N_{m-1}+2}, x^{\mathrm{O}}_{N_1}) & \cdots & M(s^{\mathrm{O}}_{N}, x^{\mathrm{O}}_{N_1}) \end{bmatrix}_{N_1 \times N_m} \tag{41}$$

$$[M^{\mathrm{O}}_{N1}] = \begin{bmatrix} M(s_1^{\mathrm{O}}, x^{\mathrm{O}}_{N_1+\cdots+N_{m-1}+1}) & M(s_2^{\mathrm{O}}, x^{\mathrm{O}}_{N_1+\cdots+N_{m-1}+1}) & \cdots & M(s^{\mathrm{O}}_{N_1}, x^{\mathrm{O}}_{N_1+\cdots+N_{m-1}+1}) \\ M(s_1^{\mathrm{O}}, x^{\mathrm{O}}_{N_1+\cdots+N_{m-1}+2}) & M(s_2^{\mathrm{O}}, x^{\mathrm{O}}_{N_1+\cdots+N_{m-1}+2}) & \cdots & M(s^{\mathrm{O}}_{N_1}, x^{\mathrm{O}}_{N_1+\cdots+N_{m-1}+2}) \\ \vdots & \vdots & \ddots & \vdots \\ M(s_1^{\mathrm{O}}, x^{\mathrm{O}}_{N}) & M(s_2^{\mathrm{O}}, x^{\mathrm{O}}_{N}) & \cdots & M(s^{\mathrm{O}}_{N_1}, x^{\mathrm{O}}_{N}) \end{bmatrix}_{N_m \times N_1} \tag{42}$$

$$[M^{\mathrm{O}}_{NN}]$$

$$= \begin{bmatrix} -\left[\sum_{j=N_1+\cdots+N_{m-1}+1}^{N} M(s_j^{\mathrm{I}}, x^{\mathrm{I}}_{N_1+\cdots+N_{m-1}+1}) - M(s^{\mathrm{O}}_{N_1+\cdots+N_{m-1}+1}, x^{\mathrm{O}}_{N_1+\cdots+N_{m-1}+1})\right] & \cdots & M(s^{\mathrm{O}}_{N_1+\cdots+N_{m-1}+1}, x^{\mathrm{O}}_{N}) \\ \vdots & \ddots & \vdots \\ M(s^{\mathrm{O}}_{N}, x^{\mathrm{O}}_{N_1+\cdots+N_{m-1}+1}) & \cdots & -\left[\sum_{j=N_1+\cdots+N_{m-1}+1}^{N} M(s_j^{\mathrm{I}}, x^{\mathrm{I}}_{N}) - M(s^{\mathrm{O}}_{N}, x^{\mathrm{O}}_{N})\right] \end{bmatrix}_{N_m \times N_m} \tag{43}$$

DOI: 10.1002/nme

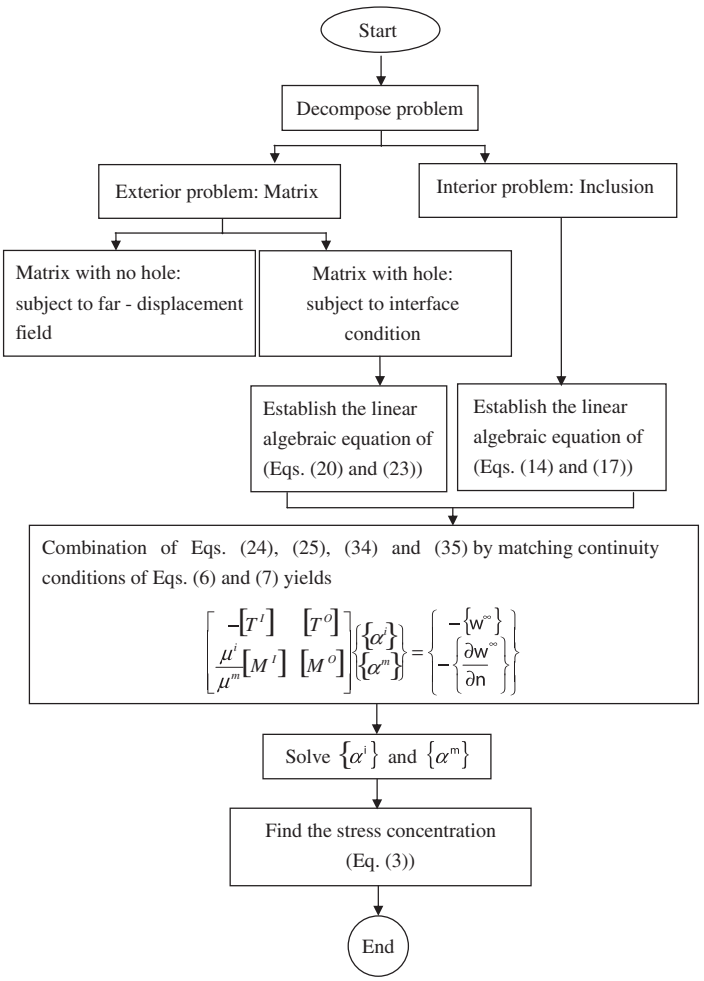

Figure 5. Flowchart of solution procedures.

2.2.4. Construction of influence matrices for antiplane shear problems. Substituting Equations (24), (25), (34) and (35) into Equations (6) and (7), the linear algebraic system for the antiplane shear problem can be obtained as follows:

$$\begin{bmatrix} -[T^{\mathrm{I}}] & [T^{\mathrm{O}}] \\ \dfrac{\mu^{\mathrm{i}}}{\mu^{\mathrm{m}}}[M^{\mathrm{I}}] & [M^{\mathrm{O}}] \end{bmatrix} \begin{Bmatrix} \{\alpha^{\mathrm{i}}\} \\ \{\alpha^{\mathrm{m}}\} \end{Bmatrix} = \begin{Bmatrix} -\{w^{\infty}\} \\ -\left\{\dfrac{\partial w^{\infty}}{\partial n}\right\} \end{Bmatrix} \tag{44}$$

where w^{∞} denotes the out-of-plane elastic displacement. After Equation (44) is solved by using the linear algebraic solver, the unknown densities ($\{\alpha^{\mathrm{i}}\}$ and $\{\alpha^{\mathrm{m}}\}$) can be obtained and thereby the field solution can be obtained by using Equation (8). To provide a simple illustration of how the proposed meshless method works, the solution procedures are listed in Figure 5.

DOI: 10.1002/nme

3. NUMERICAL EXAMPLES

In order to show the accuracy and validity of the proposed method, the antiplane shear problems with multiple inclusions subjected to the remote shear are considered. Numerical examples containing two and three inclusions under the antiplane shear, respectively, are considered. The numerical results are compared with analytical solutions [7] and those of the Laurent series expansion method [5], respectively.

Case 1: Two-inclusion problem. The antiplane problem with matrix-imbedded two inclusions is sketched in Figure 6. The smaller inclusion is centered at the origin of radius r_1 and the larger inclusion of radius $r_2 = 2r_1$ is centered on the y-axis at $r_1 + r_2 + D$ ($D = 0.1r_1$). The material parameters are $\mu_0 = 1.0$, $\mu_1 = \frac{2}{3}\mu_0$, $\mu_2 = \frac{13}{7}\mu_0$ and $\tau = 1.0\,\mathrm{N\,m^{-2}}$. For sensitivity analysis of the conventional MFS on the distance between the fictitious boundary and the physical boundary, the offset distance and the condition number are chosen as the labels of the x-axis and y-axis, respectively, where the condition number denotes $\sigma_{\max}/\sigma_{\min}$, in which $\sigma_{\max}$ and $\sigma_{\min}$ are maximum and minimum singular values of influence matrices, respectively. The sensitivity analysis on the distance between fictitious and physical boundaries is shown in Figure 7. The influence matrices are more and more ill-posed when the condition number becomes larger. The convergence analysis of stress concentrations is shown in Figure 8(a) and (b). We can obtain a convergence result after distributing 200 points by using the proposed method. Stress concentrations along the boundaries of both the matrix and the smaller inclusion are plotted in Figure 9(a)–(d), respectively, by using 720 nodes. The results are compared well with analytical solutions [7]. Figure 9(a) and (b) shows the equilibrium traction along the interface between the matrix and the smaller inclusion. Comparing with Figure 9(c) and (d), it is seen that the maximum stress concentration appears when $\theta = 0^\circ$ as expected. The absolute error of stress concentration along the interface of the smaller inclusion is plotted in Figure 10(a) and (b).

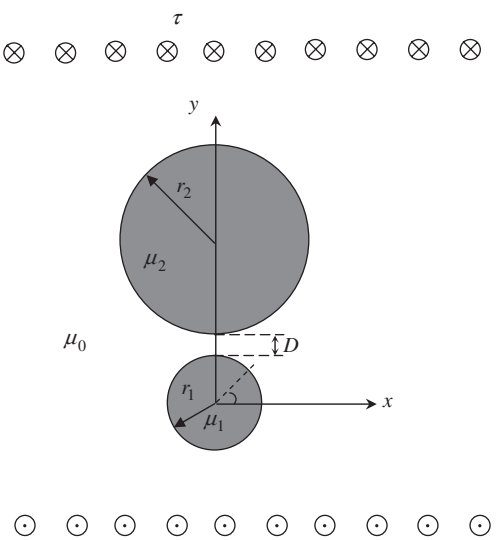

Figure 6. Problem sketch of double inclusions under antiplane shear.

DOI: 10.1002/nme

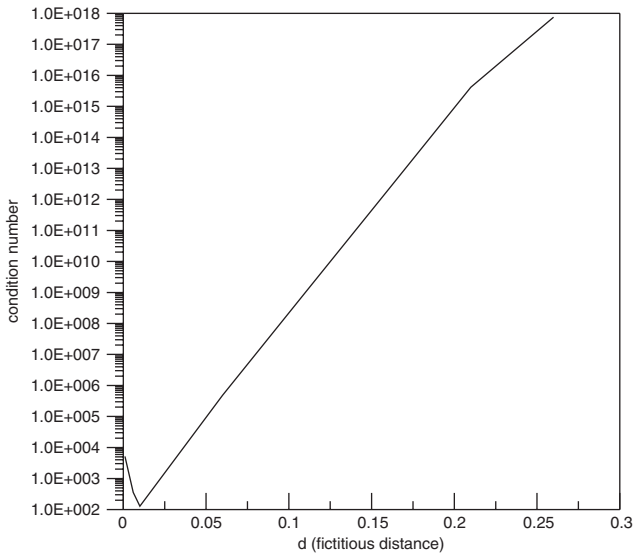

Figure 7. Sensitivity analysis on the distance between fictitious and physical boundaries by using MFS.

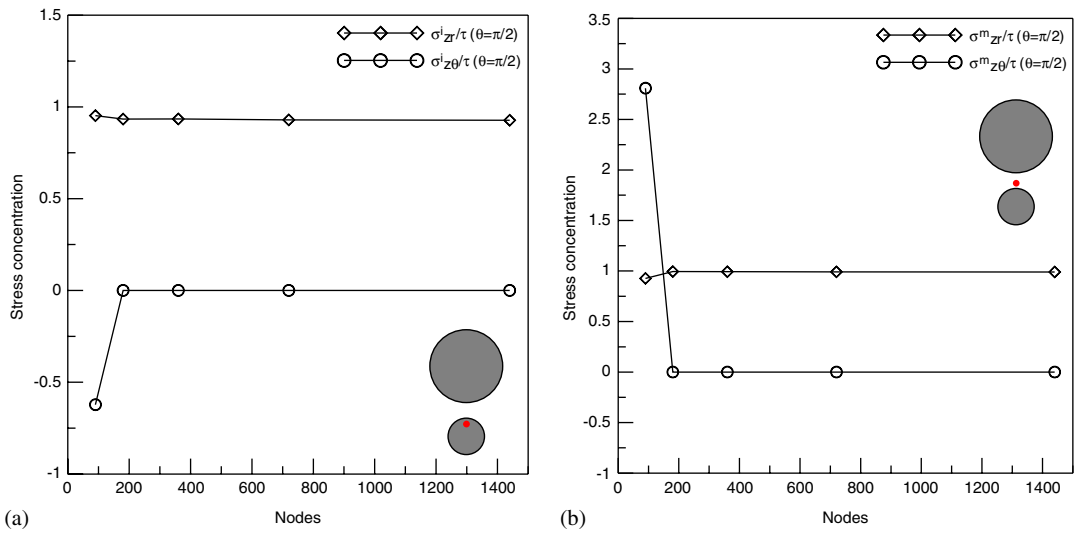

Figure 8. Convergence analysis of stress concentration in $\theta = \pi/2$: (a) inclusion and (b) matrix.

Case 2: Three-inclusion problem. A matrix imbedded three inclusions under antiplane shear is considered as shown in Figure 11. The geometry location is $D = 2r_1$. The results of convergence analysis are shown in Figure 12(a) and (b) and convergence test can be observed when the distributed boundary points are more than 250 points. The stress concentration $\sigma^{\mathrm{m}}_{z\theta}$ in the matrix around the interface of the left inclusion is evaluated as shown in Figure 13(a)–(d),

DOI: 10.1002/nme

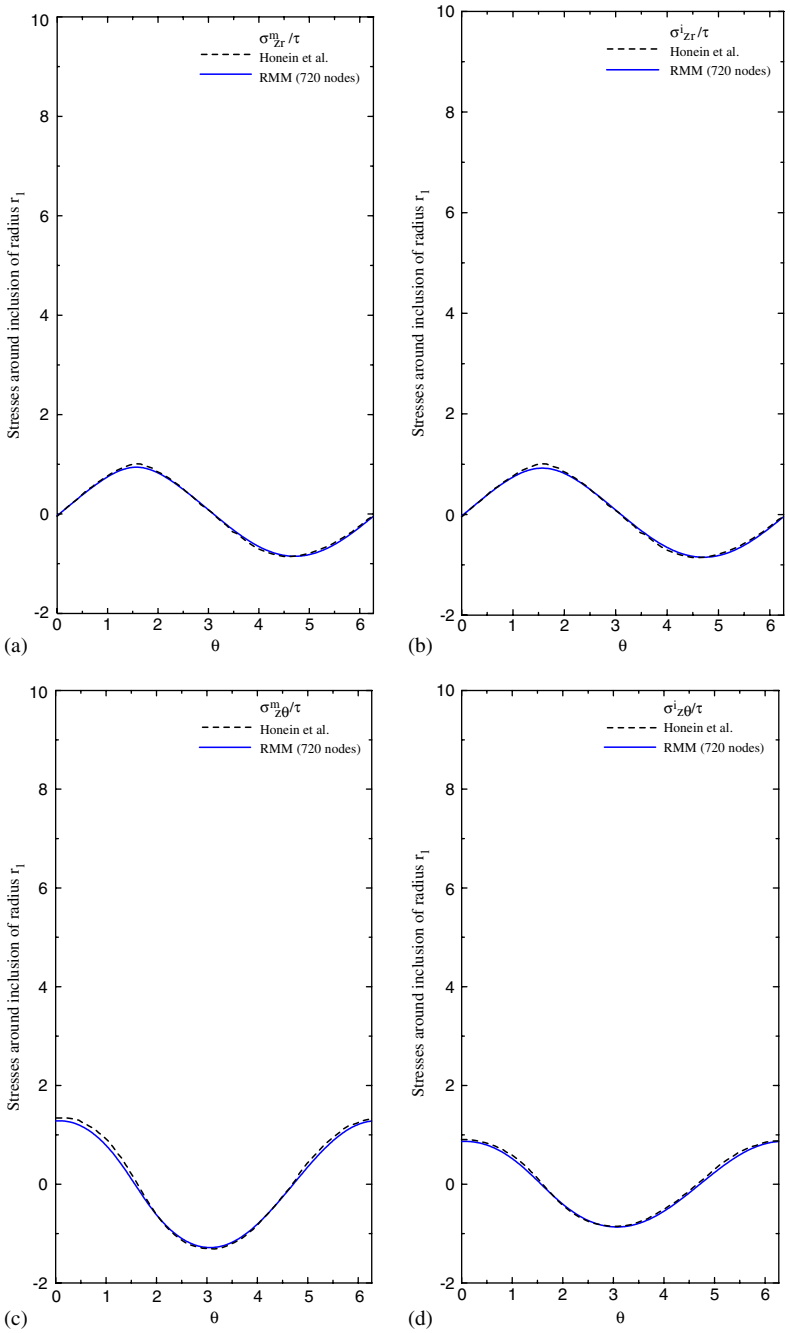

Figure 9. Stress concentration along the boundaries of both the matrix and the smaller inclusion: (a) $\sigma^{\mathrm{m}}_{zr}/\tau$; (b) $\sigma^{\mathrm{i}}_{zr}/\tau$; (c) $\sigma^{\mathrm{m}}_{z\theta}/\tau$; and (d) $\sigma^{\mathrm{i}}_{z\theta}/\tau$.

DOI: 10.1002/nme

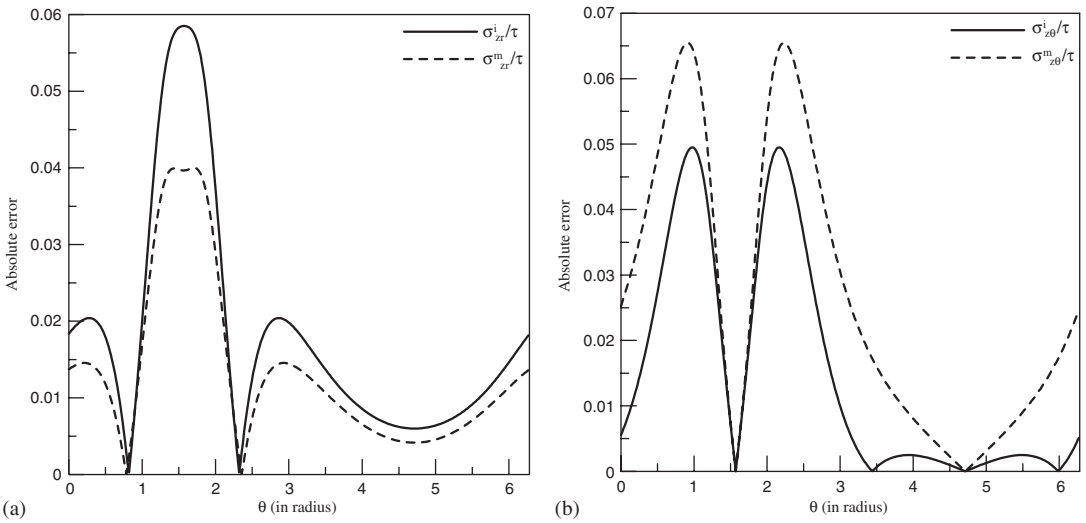

Figure 10. The absolute error of stress concentration along the boundaries of both the matrix and the smaller inclusion: (a) $\sigma^{\mathrm{m}}_{zr}/\tau$ and $\sigma^{\mathrm{i}}_{zr}/\tau$ and (b) $\sigma^{\mathrm{m}}_{z\theta}/\tau$ and $\sigma^{\mathrm{i}}_{z\theta}/\tau$.

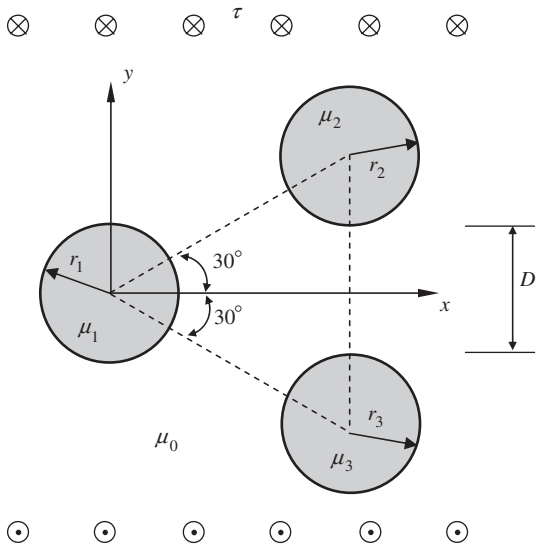

Figure 11. Problem sketch of three inclusions under antiplane shear.

respectively, by using 1080 nodes. From Figure 13(a), it is observed that the limiting case of holes ($\mu_1/\mu_0 = \mu_2/\mu_0 = \mu_3/\mu_0 = 0.0$) leads to the maximum stress concentration at $\theta = 0°$. Due to the interaction effects, it is larger than two of the single hole [7]. The stress component $\sigma_{z\theta}$ vanishes in the case of more rigid inclusions ($\mu_1/\mu_0 = \mu_2/\mu_0 = \mu_3/\mu_0 = 5.0$), which can be explained by

DOI: 10.1002/nme

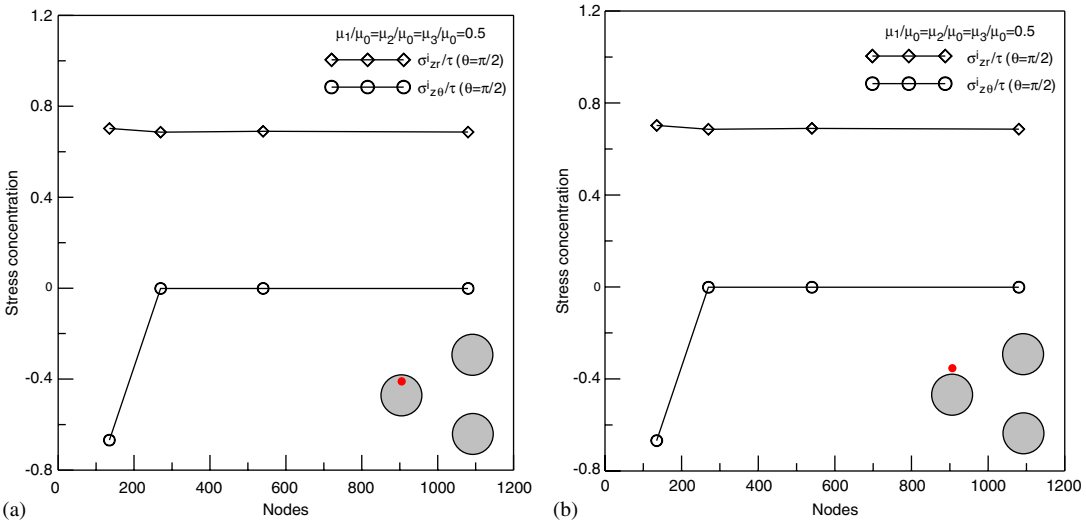

Figure 12. Convergence analysis of stress concentration in $\theta = \pi/2$: (a) inclusion and (b) matrix.

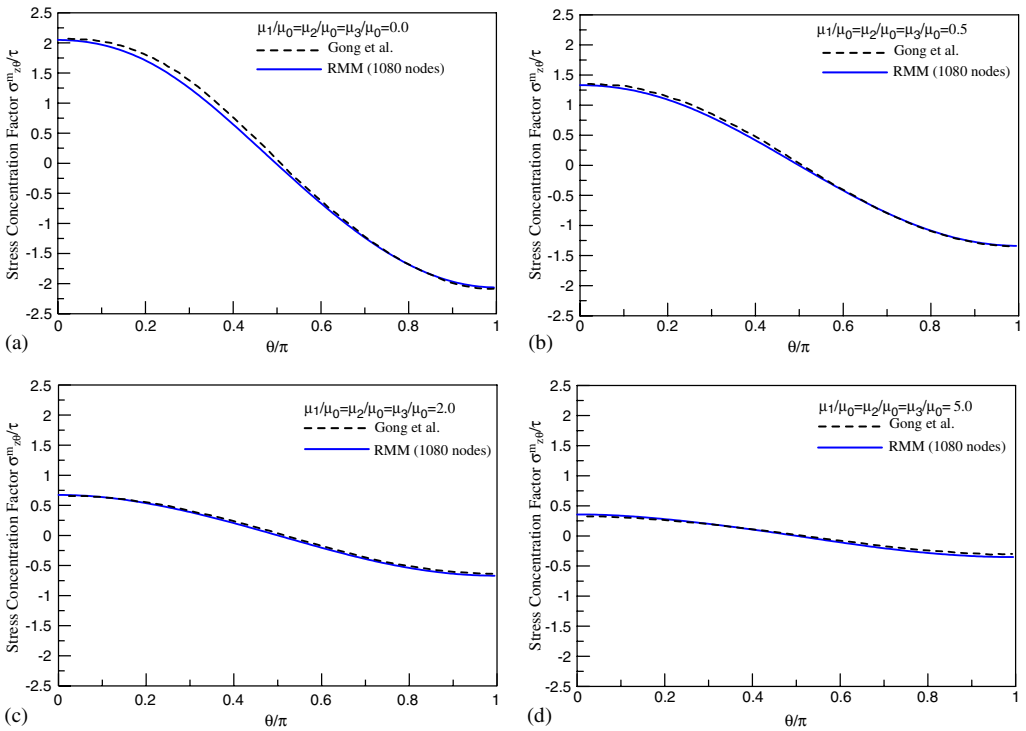

Figure 13. Stress concentration factor $\sigma^{\mathrm{m}}_{z\theta}/\tau$ along the boundaries of both the left inclusion and matrix for various shear modulus ratios: (a) $\mu_1/\mu_0 = \mu_2/\mu_0 = \mu_2/\mu_0 = 0.0$; (b) $\mu_1/\mu_0 = \mu_2/\mu_0 = \mu_2/\mu_0 = 0.5$; (c) $\mu_1/\mu_0 = \mu_2/\mu_0 = \mu_2/\mu_0 = 2.0$; and (d) $\mu_1/\mu_0 = \mu_2/\mu_0 = \mu_2/\mu_0 = 5.0$.

DOI: 10.1002/nme

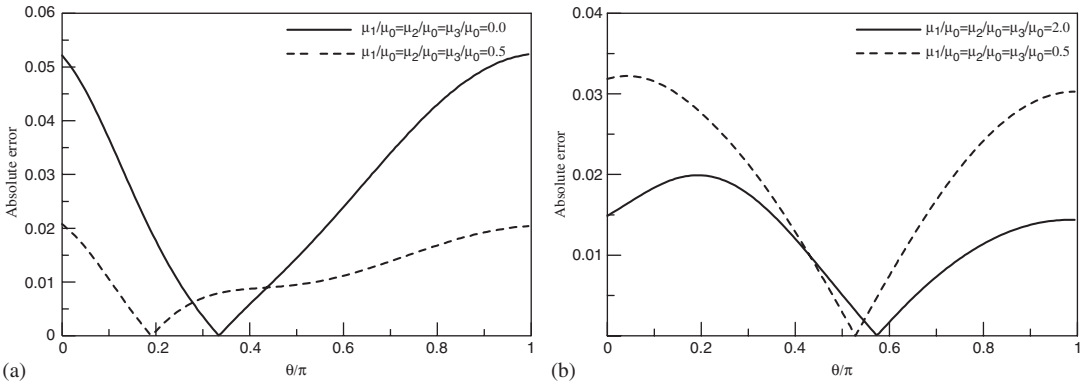

Figure 14. The absolute error result of stress concentration along the boundaries of both the matrix and the left inclusion for various shear modulus ratios: (a) $\mu_1/\mu_0 = \mu_2/\mu_0 = \mu_2/\mu_0 = 0.0$ and $\mu_1/\mu_0 = \mu_2/\mu_0 = \mu_2/\mu_0 = 0.5$ and (b) $\mu_1/\mu_0 = \mu_2/\mu_0 = \mu_2/\mu_0 = 2.0$ and $\mu_1/\mu_0 = \mu_2/\mu_0 = \mu_2/\mu_0 = 5.0$.

a general analogy between solutions for traction-free holes and those involving rigid inclusions [8]. The results are well compared with those of the Laurent series expansion method [15]. The absolute errors of stress concentration along the interface of the left inclusion for various shear modulus ratios are shown in Figure 14(a) and (b).

4. CONCLUSIONS

In this study, we extended the RMM approach to solve antiplane shear problems with multiple inclusions. Only boundary nodes on the real boundary are required. The major difficulty in the coincidence of the source and collocation points in the conventional MFS is then circumvented. Furthermore, the controversy of the fictitious boundary outside the physical domain by using the conventional MFS no longer exists. Although it results in the singularity and hypersingularity due to the use of double-layer potentials, the finite values of the diagonal terms for the influence matrices have been extracted out by employing the regularization technique. The numerical results by applying the developed program agreed very well with the analytical solution and those of the Laurent series expansion method.

ACKNOWLEDGEMENTS

Financial support from the National Science Council under Grant No. NSC-95-2221-E-464-003-MY3 for the first author is gratefully acknowledged.

REFERENCES

1. Bird MD, Steele CR. A solution procedure for Laplace's equation on multiply-connected circular domains. *Journal of Applied Mechanics* (ASME) 1992; **59**:398–404.
2. Budiansky B, Carrier GF. High shear stresses in stiff-fiber composites. *Journal of Applied Mechanics* (ASME) 1984; **51**:733–735.

DOI: 10.1002/nme

3. Chao CK, Young CW. On the general treatment of multiple inclusions in antiplane elastostatics. *International Journal of Solids and Structures* 1998; **35**:3573–3593.
4. Chen JT, Wu AC. Null-field approach for multi-inclusion problem under antiplane shear. *Journal of Applied Mechanics* (ASME) 2007; **74**:469–487.
5. Gong SX. Antiplane interaction among multiple circular inclusions. *Mechanics Research Communications* 1995; **22**:257–262.
6. Goree JG, Wilson Jr HB. Transverse shear loading in an elastic matrix containing two circular cylindrical inclusions. *Journal of Applied Mechanics* (ASME) 1967; **34**:511–513.
7. Honein E, Honein T, Herrmann G. On two circular inclusions in harmonic problems. *Quarterly of Applied Mathematics* 1992; **50**:479–499.
8. Sendeckyj GP. Multiple circular inclusion problems in longitudinal shear deformation. *Journal of Elasticity* 1971; **1**:83–86.
9. Steif PS. Shear stress concentration between holes. *Journal of Applied Mechanics* (ASME) 1989; **56**:719–721.
10. Zimmerman RW. Second-order approximation for the compression of an elastic plate containing a pair of circular holes. *Zeitschrift fur Angewandte Mathematik und Mechanik* 1988; **68**:575–577.
11. Sladek V, Sladek J, Atluri SN, Van Keer R. Numerical integration of singularities in meshless implementation of local boundary integral equations. *Computational Mechanics* 2000; **25**:394–403.
12. Sladek J, Sladek V. A meshless method for large deflection of plates. *Computational Mechanics* 2003; **30**:155–163.
13. Chen W, Hon YC. Numerical investigation on convergence of boundary knot method in the analysis of homogeneous Helmholtz, modified Helmholtz, and convection–diffusion problems. *Computer Methods in Applied Mechanics and Engineering* 2003; **192**:1859–1875.
14. Chen W, Tanaka M. A meshfree integration-free and boundary-only RBF technique. *Computers and Mathematics with Applications* 2002; **43**:379–391.
15. Hon YC, Chen W. Boundary knot method for 2D and 3D Helmholtz and convection–diffusion problems under complicated geometry. *International Journal for Numerical Methods in Engineering* 2003; **56**:1931–1948.
16. Chen JT, Chang MH, Chen KH, Lin SR. The boundary collocation method with meshless concept for acoustic eigenanalysis of two-dimensional cavities using radial basis function. *Journal of Sound and Vibration* 2002; **257**:667–711.
17. Zerroukat M, Djidjeli K, Charafi A. Explicit and implicit meshless methods for linear advection–diffusion-type partial differential equations. *International Journal for Numerical Methods in Engineering* 2000; **48**:19–35.
18. Zerroukat M, Power H, Chen CS. A numerical method for heat transfer problems using collocation and radial basis functions. *International Journal for Numerical Methods in Engineering* 1998; **42**:1263–1278.
19. Kang SW. Free vibration analysis of arbitrarily shaped plates with a mixed boundary condition using non-dimensional dynamic influence functions. *Journal of Sound and Vibration* 2002; **256**:533–549.
20. Kang SW, Lee JM. Application of free vibration analysis of membranes using the non-dimensional dynamic influence function. *Journal of Sound and Vibration* 2000; **234**:455–470.
21. Chen CS, Golberg MA, Hon YC. The method of fundamental solutions and quasi-Monte-Carlo method for diffusion equations. *International Journal for Numerical Methods in Engineering* 1998; **43**:1421–1435.
22. Tsai CC, Young DL, Cheng AHD. Meshless BEM for three-dimensional Stokes flows. *Computer Modeling in Engineering and Science* 2002; **3**:117–128.
23. Cheng AHD, Cabral JJSP. Direct solution of ill-posed boundary value problems by radial basis function collocation method. *International Journal for Numerical Methods in Engineering* 2005; **64**:45–64.
24. Cheng AHD, Young DL, Tsai CC. The solution of Poisson's equation by iterative DRBEM using compactly supported, positive definite radial basis function. *Engineering Analysis with Boundary Elements* 2000; **24**:549–557.
25. Fairweather G, Karageorghis A. The method of fundamental solutions for elliptic boundary value problems. *Advances in Computational Mathematics* 1998; **9**:69–95.
26. Karageorghis A. The method of fundamental solutions for the calculation of the eigenvalues of the Helmholtz equation. *Applied Mathematics Letters* 2001; **14**:837–842.
27. Kupradze VD, Aleksidze MA. The method of functional equations for the approximate solution of certain boundary value problems. *U.S.S.R. Computational Mathematics and Mathematical Physics* 1964; **4**:199–205.
28. Zhang YX, Tan YJ. Solve partial differential equations by meshless subdomains method combined with RBFs. *Applied Mathematics and Computation* 2006; **174**:700–709.
29. Zhang Y. Solve partial differential equations by two or more radial basis functions. *Applied Mathematics and Computation* 2006; **181**:793–801.
30. Chen KH, Kao JH, Chen JT, Young DL, Lu MC. Regularized meshless method for multiply-connected-domain Laplace problems. *Engineering Analysis with Boundary Elements* 2006; **30**:882–896.

DOI: 10.1002/nme

31. Young DL, Chen KH, Lee CW. Novel meshless method for solving the potential problems with arbitrary domain. *Journal of Computational Physics* 2005; **209**:290–321.
32. Young DL, Chen KH, Lee CW. Singular meshless method using double layer potentials for exterior acoustics. *The Journal of the Acoustical Society of America* 2005; **119**:96–107.
33. Aparicio Acosta FM. Radial basis function and related models: an overview. *Signal Processing* 1995; **45**:37–58.
34. Azevedo Leitao VM. RBF-based meshless methods for 2D elastostatic problems. *Engineering Analysis with Boundary Elements* 2004; **28**:1271–1281.
35. Golbabai A, Seifollahi S. Numerical solution of the second kind integral equations using radial basis function networks. *Applied Mathematics and Computation* 2006; **174**:877–883.
36. Golberg MA, Chen CS, Bowman H. Some recent results and proposals for the use of radial basis functions in the BEM. *Engineering Analysis with Boundary Elements* 1999; **23**:285–296.
37. Hu HY, Li ZC, Cheng AHD. Radial basis collocation methods for elliptic boundary value problems. *Computers and Mathematics with Applications* 2005; **50**:289–320.
38. Larsson E, Fornberg B. A numerical study of some radial basis function based solution methods for elliptic PDEs. *Computers and Mathematics with Applications* 2003; **46**:891–902.
39. Platte RB, Dmscoll TA. Computing eigenmodes of elliptic operators using radial basis functions. *Computers and Mathematics with Applications* 2004; **48**:561–576.

DOI: 10.1002/nme